Alternating air-medium exposure in rotating bioreactors optimizes cell metabolism in 3D novel tubular scaffold polyurethane foams

Claudia Tresoldi[1], Ilaria Stefani[1], Gaia Ferracci[1], Serena Bertoldi[1,2], Alessandro F. Pellegata[1], Silvia Farè[1,2], Sara Mantero[1,2]

[1] Department of Chemistry, Materials, and Chemical Engineering "Giulio Natta", Politecnico di Milano, Milan - Italy
[2] INSTM Local Unit, Politecnico di Milano, Milan - Italy

Claudia Tresoldi and Ilaria Stefani contributed equally to this work.

ABSTRACT

Background: In vitro dynamic culture conditions play a pivotal role in developing engineered tissue grafts, where the supply of oxygen and nutrients, and waste removal must be permitted within construct thickness. For tubular scaffolds, mass transfer is enhanced by introducing a convective flow through rotating bioreactors with positive effects on cell proliferation, scaffold colonization and extracellular matrix deposition. We characterized a novel polyurethane-based tubular scaffold and investigated the impact of 3 different culture configurations over cell behavior: dynamic (i) single-phase (medium) rotation and (ii) double-phase exposure (medium-air) rotation; static (iii) single-phase static culture as control.
Methods: A new mixture of polyol was tested to create polyurethane foams (PUFs) as 3D scaffold for tissue engineering. The structure obtained was morphologically and mechanically analyzed tested. Murine fibroblasts were externally seeded on the novel porous PUF scaffold, and cultured under different dynamic conditions. Viability assay, DNA quantification, SEM and histological analyses were performed at different time points.
Results: The PUF scaffold presented interesting mechanical properties and morphology adequate to promote cell adhesion, highlighting its potential for tissue engineering purposes. Results showed that constructs under dynamic conditions contain enhanced viability and cell number, exponentially increased for double-phase rotation; under this last configuration, cells uniformly covered both the external surface and the lumen.
Conclusions: The developed 3D structure combined with the alternated exposure to air and medium provided the optimal in vitro biochemical conditioning with adequate nutrient supply for cells. The results highlight a valuable combination of material and dynamic culture for tissue engineering applications.
Keywords: Biomaterials, Bioreactors, Dynamic culture, Tissue engineering

Introduction

Noncommunicable diseases, mainly cardiovascular diseases, cancers, diabetes, obesity and chronic respiratory diseases, are the main causes of death in high-income countries. Cardiovascular pathologies account for 17.3 million deaths annually, followed by malignant tumors with 7.6 million, respiratory diseases (4.2 million) and diabetes (1.3 million) (1).

Considering the 12 major causes of death in the world, more than half regard hollow organ pathologies (2, 3).

Over the last 50 years, transplantation of a wide variety of tissues and organs, reconstructive surgical techniques and replacement with artificial devices have significantly enhanced patient life expectancy and quality of life. Unfortunately, these solutions suffer from many limitations, such as donor shortage and requirement for lifelong immunosuppressive assumption, increased risk of infections, undesirable side effects and, in some cases, finite durability (4-6).

This situation led to the tissue engineering (TE) approach to develop in vitro cellularized functional substitutes able to restore or improve tissue and organ activities (6, 7). In this regard, bioreactor-scaffold complexes, together with autologous cells, are pivotal to obtaining a functional implantable tissue engineered graft.

To reproduce in vitro optimal biochemical and biomechanical conditioning, the optimization of the mass transport

within cultured three-dimensional (3D) scaffolds is necessary. For the regeneration of complex hollow constructs, mass transfer can be enhanced by a convective flow obtained through dynamic culture within longitudinal rotation bioreactors. These devices allow an increased removal of catabolites and an optimized nutrient diffusion in 3D scaffolds, compared with static culture. In this last condition, an adequate oxygen supply reaches a maximum scaffold depth of 100 μm (8-10). A controlled increase in rotational speed, inducing different laminar shear stress, can positively influence uniform cell proliferation, a better colonization and extracellular matrix deposition (ECM) throughout the scaffold thickness (11-14).

In addition to the dynamic culture conditions, scaffold architecture and biomaterial chemistry affect grafts mechanical properties, mass transport, cellular response and interaction with the scaffold (15, 16). A controlled pore size and an increased pore interconnection allow cell migration, proliferation and tissue growth, promoting also the postimplant angiogenesis throughout the scaffold (17).

Synthetic scaffolds are very promising for hollow tissue regeneration because of the ease in controlling their architecture, surface chemistry and mechanical properties, in relation to the targeted tissue (15, 16, 18, 19), by adjusting production process parameters (20, 21). Among synthetic polymers used for tubular tissue-engineered structures (14, 16, 22), polyurethane foams (PUFs) are very interesting for 3D scaffold applications (i.e., bone, cartilage and soft tissues) (23-26) thanks to their high tunable process properties that can modify pore size, interconnectivity and mechanical properties.

At present, despite the relevance of suitable supply of oxygen and nutrients with 3D scaffolds throughout dynamic bioreactors, in the literature there is no evidence about a generalization of convective flow as both biochemical and mechanical stimulus in in vitro dynamic cultures. Moreover, the differences in cell metabolism, viability and colonization of a tubular support between a double-phase (medium-air) (8) in comparison with a single-phase (medium only), or static incubation of the construct, have never been reported in the literature.

Thus, in the present work we demonstrated the importance of the convective flow induced by longitudinal rotation for tubular constructs. Firstly, we investigated a new formulation of PUF scaffold for application in tubular TE, characterizing the mechanical and biological properties. Then, we analyzed the effect of longitudinal rotation on cell activity into the PUF scaffold under different configurations of in vitro culture. We compared 2 diverse dynamic conditioning cases: (i) single-phase (medium) rotation and (ii) double-phase exposure (medium-air) rotation. A single-phase exposure (only culture medium) in static condition was used as a control. The ultimate aim was to identify the optimal dynamic culture conditions in terms of cell proliferation, metabolism and colonization, demonstrating that the double-phase exposure positively affects cell behavior.

Materials and methods

Polyurethane foam synthesis

PUFs were synthesized following a previously described 1-step bulk polymerization method (27, 28), using water as

TABLE I - Components of the polyol mixture and their main properties

Component	Functionality	OH number (mgKOH/g)	MW (Da)	Producer
Desmophen® 10WF18	2.7	27.6	5,500	Bayer
Desmophen® 7619W	≈ 3	128.8	-	Bayer
Desmophen® 4051B	≈ 4	467.4	480	Bayer
1-4, Butandiol	2	1,245.0	-	Sigma-Aldrich
Ethylene glycol (EG)	2	1,810.0	-	Sigma-Aldrich
Potassium acetate in EG	-	1,810.0	-	Sigma-Aldrich
DABCO 33-LV	-	560.0	-	Air Products

MW = molecular weight; OH = hydroxy group.

an expanding agent and iron-acetylacetonate (FeAA) as catalyst. Briefly, a new polyol mixture was ad hoc prepared using the reagents listed in Table I. FeAA (0.001% w/w_{polyol}), distilled water (2% w/w_{polyol}) and the appropriate amount of isocyanate (stoichiometric ratio of OH/NCO = 100/73) and methylene diphenyl diisocyanate prepolymer (Desmodur® PF, Bayer, Germany; −NCO = 23.0% ± 0.5%) were added to the polyol mixture, mixed with a mechanical stirrer for 60 seconds and finally poured into a custom-made poly(methylmethacrylate) mold (V = 500 cm³). The expanding reaction took place at room temperature (RT). Foams were extracted from the mold after 72 hours, and the superficial compact skins were removed to obtain a homogeneous porous structure. Then foams were postcured at RT for 7 days. The synthesized structures were sliced selecting 2 different heights (h = 3 mm and h = 6 mm), purified by a 48-hour immersion in absolute ethanol at RT, and subsequently carefully dried in a fume hood before characterization.

Scaffold morphological characterization

Scanning electron microscopy observation

Samples morphology was investigated by scanning electron microscopy (SEM; Stereoscan 360; Cambridge Instruments) at 15-18 keV and working distance of 7.5-12 mm. Before analysis, the samples were sputter-coated with a 20-nm layer of gold (Sputter Coater S150B; Edwards). The images were acquired at 25× and 100× magnification.

Micro-computed tomography

Three PUF specimens (Ø = 6 mm, h = 6 mm) were individually analyzed. Porosity, average pore size, pore size distribution and pore interconnection were evaluated by micro-computed tomography (micro-CT) analysis using a 1172 micro-CT imaging system (Skyscan; Aartselaar) following a
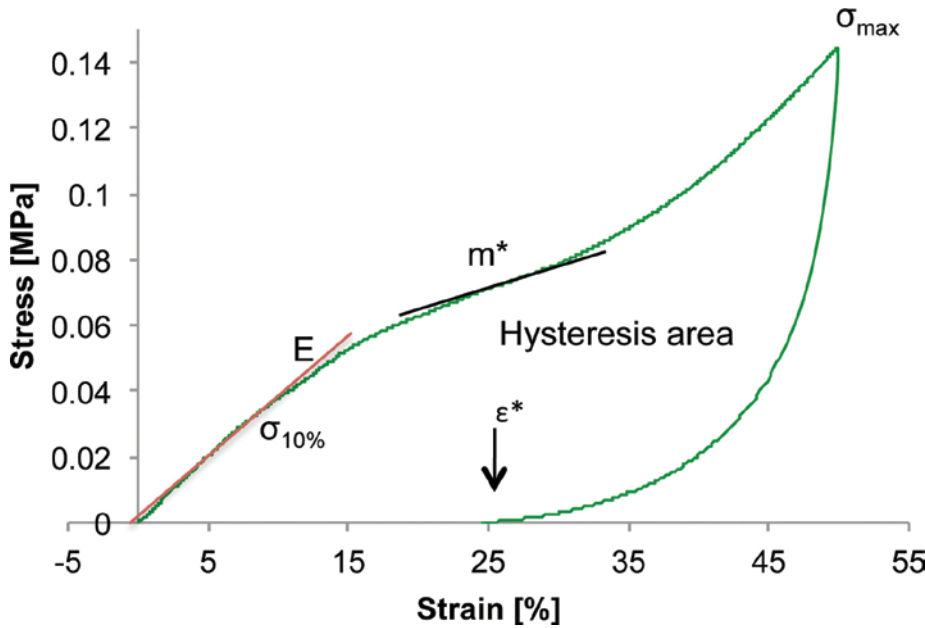
Fig. 1 - Representative stress–strain curve obtained by compressive test of polyurethane foam (PUF) samples. Mechanical parameters reported are tangent modulus (E), collapse modulus (m*), stress at 10% deformation ($\sigma_{10\%}$), maximum stress (σ_{max}), residual deformation (ε*) and hysteresis area.

previously described protocol (28). 3D reconstruction of the internal pore morphology was carried out using axial bitmap images and analyzed by CTan software (Skyscan; Aartselaar). The gray scale threshold was set between 55 and 230, removing all objects smaller than 400 voxels and not connected to the 3D model. To eliminate potential edge effects, the cylindrical volume of interest (VOI) was selected in the center of the specimen ($\emptyset$ = 3 mm, h = 1.5 mm). Scaffold porosity was then calculated as:

Porosity = 100% − vol% of binarized object   Eq. [1]

where *vol% of binarized object* is the total volume of scaffold, calculated as the product between the voxel volume and the voxel number of binarized solid elements contained in the VOI.

A shrink-wrap process was performed between two 3D measurements to shrink the outside boundary of the VOI in a scaffold through any openings whose size was equal to or larger than a fixed threshold value (29). Interconnectivity was calculated as follows:

$$Interconnectivity = \frac{V - V_{shrink-wrap}}{V - V_m} \times 100 \qquad \text{Eq. [2]}$$

where V is the total volume of the VOI, $V_{shrink-wrap}$ is the VOI volume after shrink-wrap processing and V_m is the volume of the sample material. The interconnective pore size was hereby called the *cutoff pore diameter*.

Water uptake

Dried samples ($\emptyset$ = 4 mm, h = 3 mm) were immersed in deionized water (dH$_2$O) at 37°C; at each time point (0.5, 2, 6, 24 hours, and every 24 hours up to the 25th day). Specimens were drawn from the water, wiped with filter paper to re-move excess liquid, and weighed. The water uptake (W.U.%) was calculated according to the Eq. [3]:

$$W.U.\% = \frac{W_t - W_o}{W_o} \times 100 \qquad \text{Eq. [3]}$$

where W_o is the dry weight and W_t is the wet weight at the time point *t*.

Mechanical compression characterization

The mechanical properties of PUFs were investigated using a dynamic mechanical analyzer (DMA Q800; TA Instruments). Compression tests were performed on disk-shaped specimens ($\emptyset$ = 4 mm, h = 3 mm) in dry (n = 3) and hydrated (n = 3) condition by applying a preload of 0.1 N; after an isotherm at 37°C for 5 minutes, a deformation ramp of 2.5%/min up to 50% deformation of the initial thickness was applied, followed by a deformation ramp of 5%/min down to 0.1% deformation. Specimens for hydrated tests were previously immersed in dH$_2$O to reach the swelling plateau. Experiments were carried out in immersion in a custom-made chamber, to maintain the sample in hydrated condition for the whole test time Tangent modulus (E), collapse modulus (m*), stress at 10% deformation ($\sigma_{10\%}$), maximum stress (σ_{max}), residual deformation (ε*) and hysteresis area (I), related to energy dispersion, were drawn from the stress–strain curve (Fig. 1).

In vitro biological characterization

Cell expansion

Cells from a murine fibroblast cell line (L929, 85011425; Sigma-Aldrich) were cultured and expanded in Dulbecco's modified Eagle's medium (DMEM 5671; Sigma-Aldrich), with 10% fetal bovine serum (FBS, F7524; Sigma-Aldrich), 1% HEPES
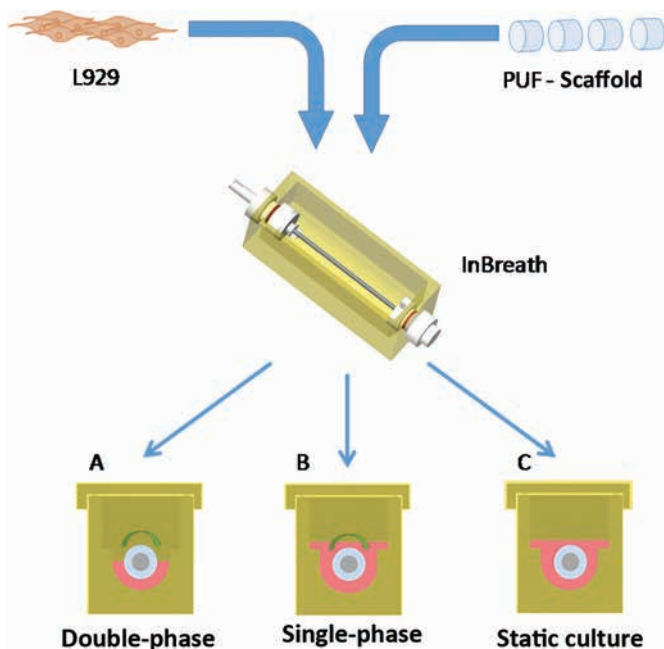
Fig. 2 - Scheme of the experimental conditions in the InBreath bioreactor. Double-phase (**A**) scaffolds were under longitudinal rotation and alternately exposed to air and culture medium. Single-phase (**B**) scaffolds were under longitudinal rotation and exposed only to culture medium. Static culture (control; (**C**) scaffolds were cultivated in static conditions and exposed only to culture medium. Light blue represents the tubular polyurethane foam (PUF) scaffold, gray indicates the plain stainless steel mandrel and rose indicates culture medium.

(H3375; Sigma-Aldrich), 1% sodium pyruvate (P2256; Sigma-Aldrich), 1% L-glutamine (G7513; Sigma-Aldrich) and 1% penicillin-streptomycin (P0781; Sigma-Aldrich).

Scaffold preparation and disinfection

For static culture, PUF samples (Ø = 8 mm, h=6 mm) were cut using a biopsy punch. For dynamic culture, cylindrical samples were prepared with an inner diameter of 4 mm. All PUF samples were disinfected by immersion in 70% v/v ethanol solution (EtOH) for 30 minutes, subsequently washed with sterile phosphate buffered saline (PBS) 4 times and left drying overnight in a biosafety cabinet.

Biological assessment

Biological tests were performed under static culture conditions, to evaluate the interaction of L929 fibroblasts with PUF. L929 (seeding density = 2×10^4 cell/cm^2) were seeded on the scaffolds. Cells seeded on polystyrene culture plate (TCP) were considered as controls (Ctrl). At each time point (t = 1, 3 and 7 days) SEM and viability and DNA quantification analyses were performed.

Dynamic culture configurations

Dynamic cultures were performed as described here below, and at considered time points, different analysis were per-

formed. Sterilized cylindrical-shaped scaffolds were mounted on a plain 4 mm Ø stainless steel mandrel using surgical gloves. For the dynamic tests, 2 different conditions were examined (Fig. 2). The first (Fig. 2A) consisted of a double-phase culture (double-phase): the scaffold was half immersed in culture medium and alternatively exposed to the air and to the culture medium in a rotating bioreactor with a speed rate of 3 rpm. In the second configuration (Fig. 2B), the entire scaffold was immersed in the culture medium, with a rotation speed of 3 rpm (single-phase). In the static culture (Fig. 2C), considered as the control, the scaffold was completely covered by the culture medium (static). The bioreactor setup (Fig. 3) was suitable for tubular scaffolds and its configuration was adapted from the previous one (8); the Petri-like cap of the device was maintained as it allowed a safe and sterile exchange of the controlled air of the incubator with the inner chamber. For the single-phase and double-phase configurations, the rotation movement was transmitted through polyoxymethylene holders to the cylindrical scaffold harbor, using direct current motors (PSU 130; Lascar Electronics Ltd.).

PUF cylindrical scaffolds (5 for each time point) were seeded with L929 (density = 2×10^6 cells per specimen) by 4 cell suspension drops (10 µL/drop) every 90°. Double-phase and single-phase systems were continuously rotating at 2 rpm for 4 hours in the incubator to promote cell adhesion and for a more homogeneous cell distribution. Samples in static condition were maintained for the same time in the incubator, without any rotation. At the end of the seeding step, each bioreactor was maintained under static conditions for 24 hours, after adding 45 mL of DMEM to completely submerge the scaffolds and allow better cell adhesion. Then, 15 mL of culture medium was removed from the double-phase system to expose the superior half of the scaffold to the air. Half of the media volume was manually changed every 72 hours. Analyses were performed for 7, 14 and 21 days; for each time point, 5 samples were harvested.

Sample analyses

Cell viability assay

Cell viability was evaluated at each time point with the resazurin colorimetric assay (Alamar Blue®; Serotec Ltd, Kidlington, Oxford, UK). Samples cultured in bioreactors were transferred to a 24-well plate. Briefly, the Alamar Blue® solution was diluted at a 1:10 ratio in DMEM; 500 µL (direct cytocompatibility test) or 1 mL (dynamic culture) was added to each sample and incubated for 4 hours in the incubator. Supernatant fluorescence at 590 nm (λ = 510 nm as the reference wavelength) was measured by a Multifunction Tecan (GENios Plus).

DNA quantification

The total number of cells was estimated by DNA quantification for the static and the dynamic cultures. Samples were immersed in cell digestion buffer at 55°C overnight with 0.005 volume proteinase K, followed by a treatment with sodium acetate pH 5.2 to precipitate proteins and debris. To extract DNA, the supernatant was diluted in 98%

Fig. 3 - (**A**) Polyurethane foam (PUF) cylindrical sample, (**B**) PUF scaffolds located on a plain stainless steel mandrel in the InBreath bioreactor (8). (**C**) Bioreactor setup used for the different configuration culture systems as it is inserted in the incubator; in this picture the Petri dish–like cap, which allows for oxygen exchange with the controlled environment of the incubator while maintaining sterility of the inner chamber, is visible.

and 70% EtOH and centrifuged. The resulting DNA pellet was rehydrated with dH_2O. Total DNA was marked with SYBR® Green (S9430; Sigma-Aldrich). A calibration curve using salmon sperm (500 ng/μL) was plotted as the reference line for the extracted DNA. Fluorescence at 535 nm was measured by Tecan spectrophotometer, by analyzing each rehydrated DNA sample (100 μL each) in triplicate. Cell number was estimated considering an average DNA quantity of 7 pg/cell.

SEM observations

Microscopic investigations were performed by SEM. The specimens were fixed by immersion in a solution of 3% v/v of 50% glutaraldehyde in 0.1 M sodium cacodylate for 2 hours, and subsequently washed in 0.1 M sodium cacodylate. Later, samples were dehydrated with increasing concentrations of ethyl alcohol and finally gold sputtered. Images of inner and outer specimen surfaces were acquired at 250× magnification for samples obtained in the cytocompatibility test, and at 25× and 100× magnifications for dynamic experiments in bioreactor.

Histological analysis

To assess the extent of scaffold colonization and ECM overall deposition, histological analyses were performed on 10-μm-thick slices of the cylindrical samples (superior, middle and inferior part) for each time point and for the 3 culture configurations. PUF constructs were fixed in 4% paraformaldehyde. After treatment with sucrose (30% w/v in PBS) and a following step with a 50% tissue-freezing medium in 30% w/v sucrose solution, specimens were immersed in OCT and frozen in liquid nitrogen. Thereafter, samples were cut by a microtome and stained with hematoxylin and eosin. Histological images were acquired at 2× magnification.

Statistical analysis

Results were expressed as means and standard deviation of at least 3 samples. Two-way and multivariate analysis of variance (ANOVA) test were performed using GraphPad Prism software for Windows (GraphPad Software Inc.). A significance level of a p value <0.05 was applied.

Results

Morphological characterization of PUF scaffolds

SEM observation

The morphology of PUF observed by SEM analysis is shown in Figure 4A. PUF presented homogeneous morphology with regular round-shaped pores and size distribution, with a high pore interconnection.

Micro-CT analysis

The values of total porosity, open porosity, pore size and pore wall thickness obtained by micro-CT are reported in Table II. Values of total porosity indicated that interconnected pores occupied most of the volume of the structures. The values of the average pore size and the thickness of pore wall confirmed the qualitative observations with SEM. The percentage of accessible porosity decreased with increasing interconnection diameter, but was always at about 80%, indicating a high pore interconnection (Fig. 4B).

Water uptake

The kinetics of PUF water uptake (Fig. 4C) showed a transitory initial phase, with high water uptake rate, until reaching a plateau after 7 days. As expected, the plateau value was maintained for the test time considered, without any significant difference among the W.U.% values (p>0.05).

Mechanical characterization

In Figure 4D, representative hysteresis cycle curves of PUF specimens obtained by compressive tests performed in dry or hydrated (wet) condition are shown, and in Table III the values of the considered mechanical parameters are reported.

Comparing the curves of PUF related to the dry and wet condition, the water uptake caused a decrease in the mechanical properties, with a significant difference in the elastic modulus, $\sigma_{10\%}$, and σ_{max} values (p<0.01) (Tab. III). This decrease of the PUF mechanical properties in hydrated condition could be related to the plasticizing effect of water that causes a high flexibility and a lower mechanical strength. In addition, the significant difference in the PUF residual deformation
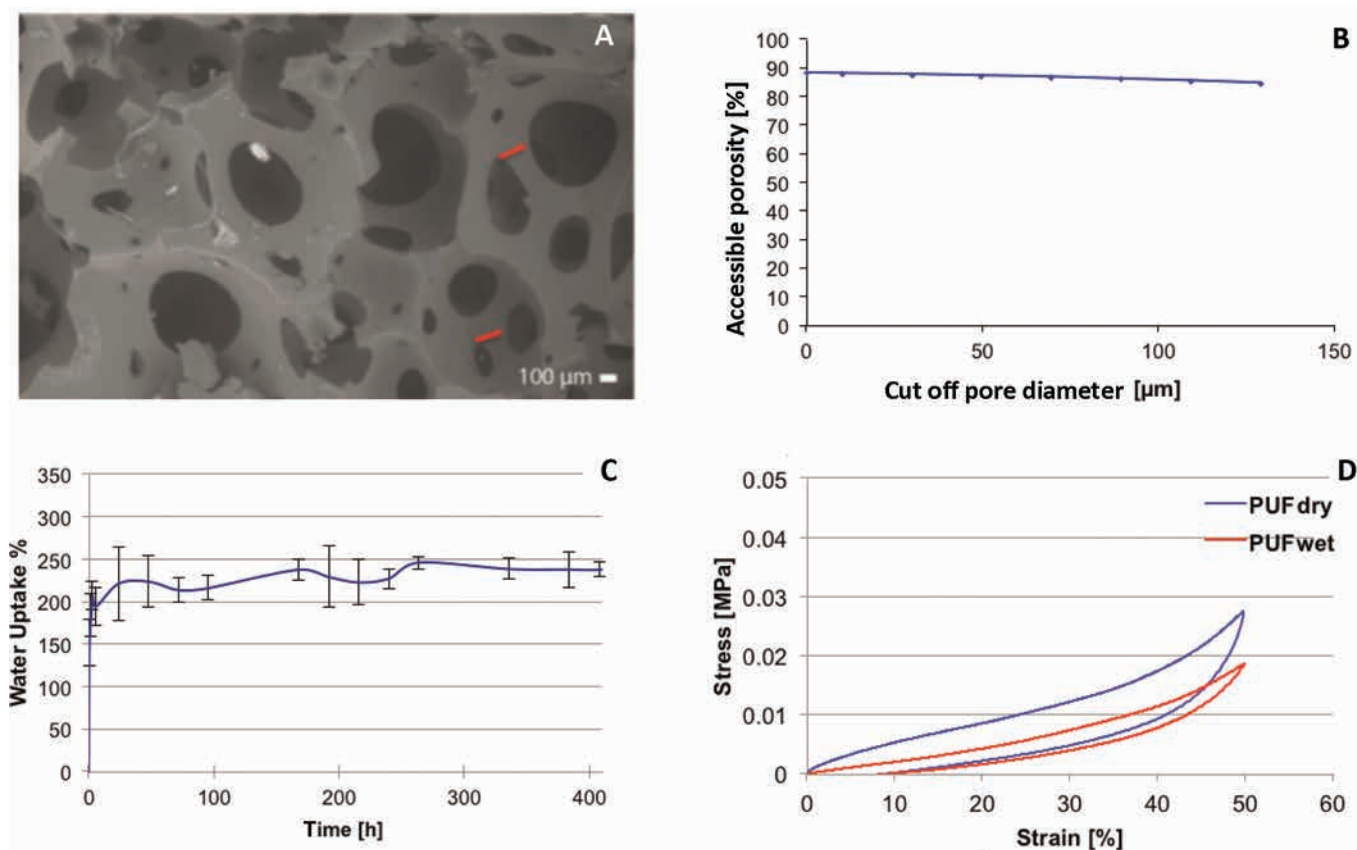
Fig. 4 - (**A**) Representative SEM images of the surface and cross-section morphology of polyurethane foam (PUF). Red arrows show high pore interconnections (scale bar: 100 μm). (**B**) Average pore size distribution obtained by micro-computed tomography analysis; pore interconnection is expressed in terms of accessible porosity at different cutoff pore diameters. (**C**) Water uptake for up to 17 days. (**D**) Representative compressive stress–strain curves of PUF tested in dry and hydrated conditions. PUF = polyurethane foam.

TABLE II - Total porosity, open porosity, average pore size and pore wall thickness for PUF analyzed by micro-CT

Total porosity (%)	Open porosity (%)	Average pore size (μm)	Pore wall thickness (μm)
89.13 ± 0.84	89.06 ± 0.84	548 ± 120	60.75 ± 4.96

micro-CT = micro-computed tomography; PUF = polyurethane foam.

(p<0.05) and hysteresis area (p<0.01) confirmed the effect of water absorption. In particular, the decrease in hysteresis area value indicated the elastic mechanical behavior of the PUF in a hydrated condition, compared with the viscoelastic behavior detected for PUF tested in a dry condition.

Biological assessment

Viability of cells on PUF scaffolds, as well as for Ctrl, was statistically increased (p<0.01), with an exponential trend, during the cell culture (Fig. 5A). No statistically significant difference was found between viability of cells on PUF and Ctrl (i.e., culture plastic) at 1-day and 3-day culture, indicating that L929 were well adherent on PUF specimens. Just after 7 days,

a statistical difference between PUF and Ctrl was evidenced. DNA quantification (Fig. 5B) confirmed the results obtained in the viability test, in that estimated cell numbers at each time point presented the same trend and the same statistical difference (p<0.01). SEM investigations (see Supplementary Figure 1, available online as supplementary material at www. jab-fm.com – SEM images of internal, external and cross-section of PUF samples for direct cytotoxicity. Scale bars = 100 μm) evidenced the morphological modification of L929 upon scaffolds. A progressive cell spreading was visible, from a rounded shape after 1 day to a well-adhesive and flattened conformation observed 7 days after seeding; cells adhered also in PUF pores below the external surface.

Dynamic culture configurations

Viability assay and DNA quantification

Values obtained from viability test and DNA quantification (Fig. 6) showed different cell responses in the 3 configurations in the bioreactor. For the static configuration, there was a stable metabolic activity for the 7-day and 14-day time points that was reduced in the last time point; DNA quantification indicated an increase in cell number from 7 days to

TABLE III - Compressive mechanical properties of PUF scaffolds

	E (MPa)	m* (MPa)	$\sigma_{10\%}$ (MPa)	σ_{max} (MPa)	ϵ^* (%)	I (J/cm³)
Dry	0.05 ± 0.00	0.03 ± 0.01	0.005 ± 0.000	0.03 ± 0.01	10.92 ± 1.01	0.32 ± 0.05
Wet	0.02 ± 0.00	0.03 ± 0.00	0.001 ± 0.000	0.02 ± 0.00	11.62 ± 1.87	0.13 ± 0.01

PUF = polyurethane foam.
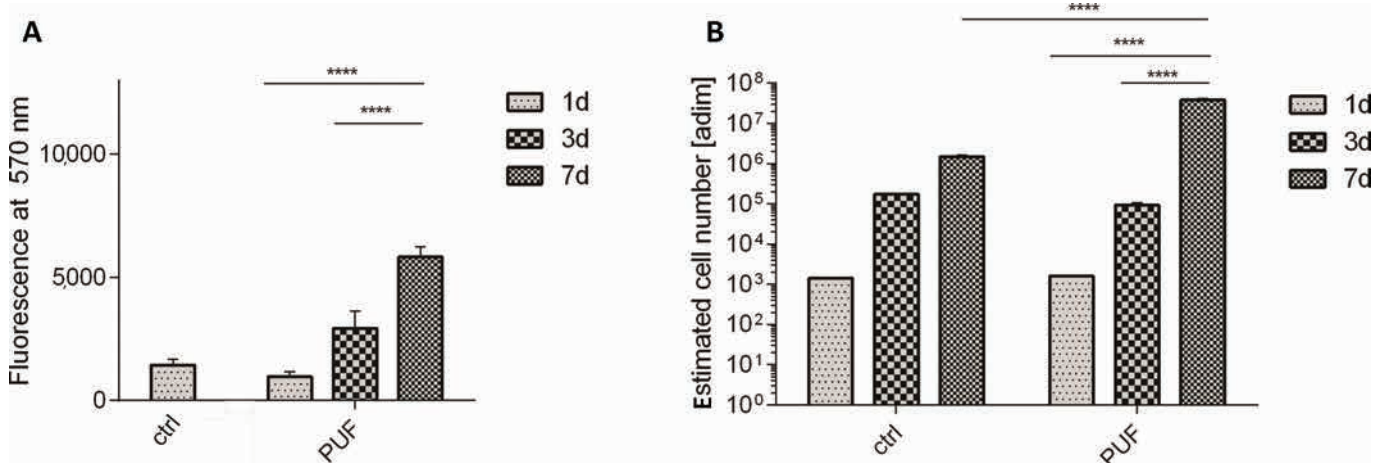
Fig. 5 - Quantitative analyses performed on polyurethane foam (PUF) scaffolds for cell attachment and growth. Three time points are reported (1, 3 and 7 days); TCP was used as control (Ctrl). (**A**) Alamar Blue assay (Ctrl day 1 only); (**B**) DNA quantification. ****p≤0.0001.
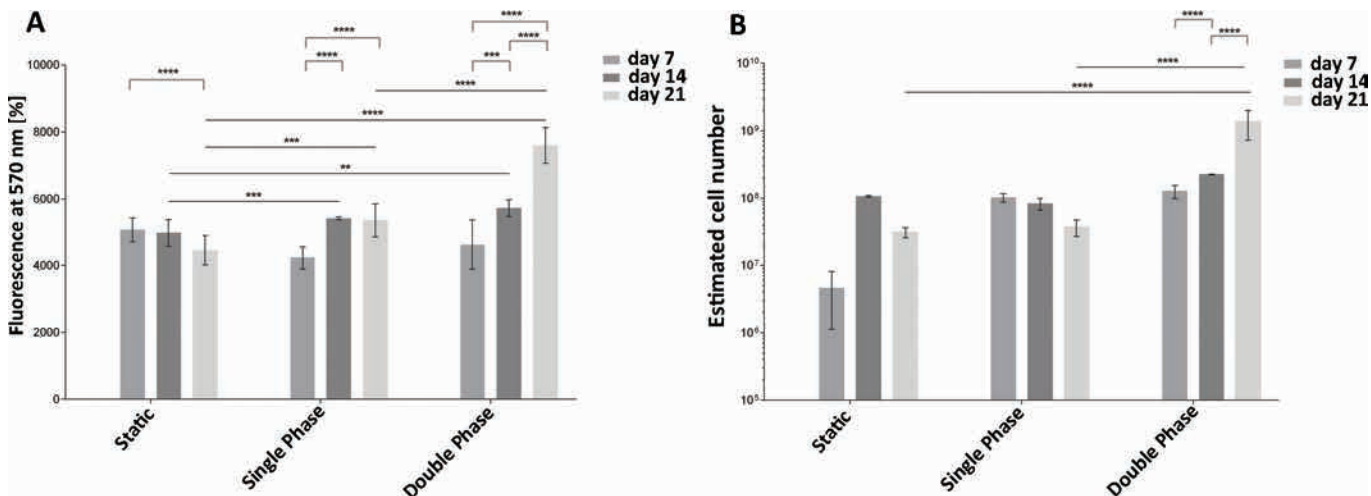
Fig. 6 - (**A**) Alamar Blue viability assay and (**B**) DNA quantification performed on polyurethane foam (PUF) samples under dynamic culture and static control conditions, for up to 21 days. *p<0.05; **p<0.005; ***p<0.0005; ****p<0.0001.

14 days, but this growth significantly slowed after 21 days of culture (p<0.05). In contrast, in the single-phase configuration, viability presented a 7-day to 14-day significant increase (p<0.01), while it became stable up to the last time point. The estimated cell number was constant throughout the culture. Focusing on the double-phase configuration, cells increased both in viability and in number, with a statistically significant increase (p<0.01) (Fig. 6).

SEM observations and histological analysis

In the static configuration (Fig. 7), cells completely covered the external surface with ECM during culture time, and formed a continuous layer, closing the smallest pores of the PUF scaffold. The internal surface was quite bare, and no cells were detectable attached to the PUF pore wall surface. In the single-phase exposure, ECM entirely covered the external
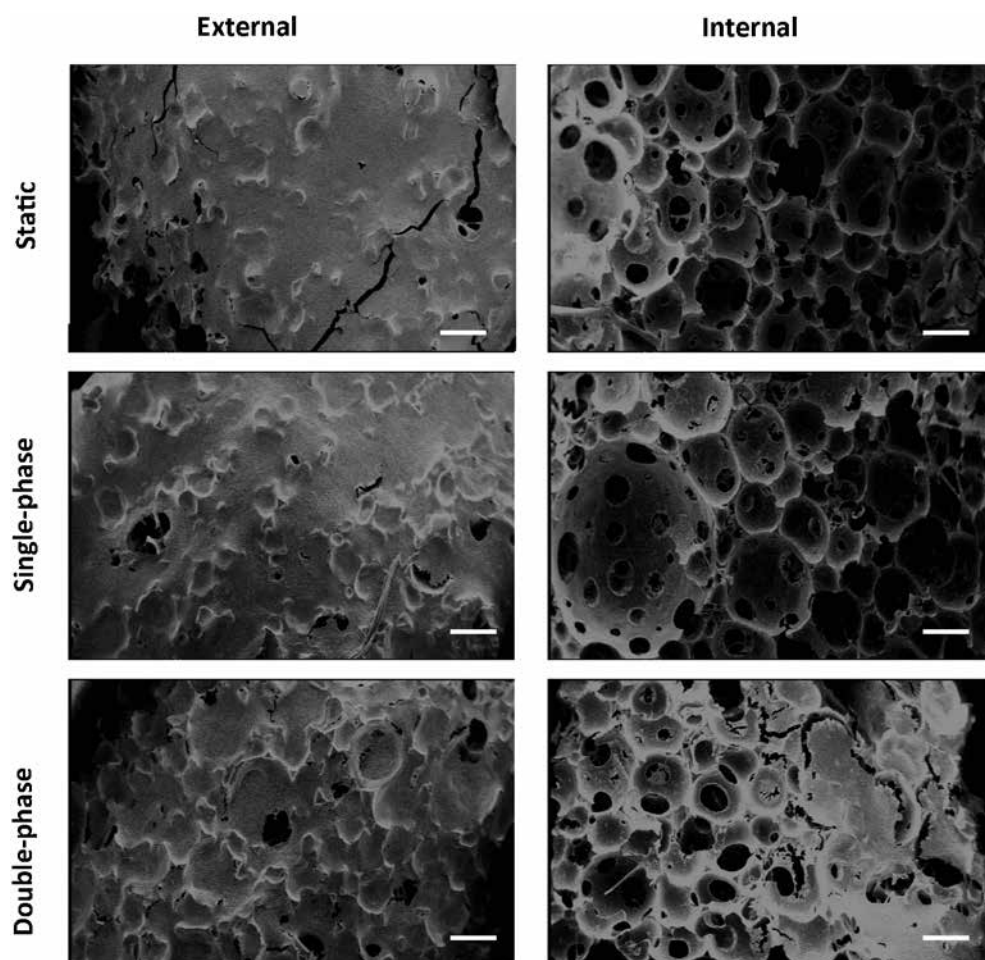
External   **Internal**

surface, closing all pores throughout the dynamic culture duration, but still the luminal side of the scaffold was scarcely populated and minimal ECM formation was noticeable in the smallest pores in the inner surface of the PUF scaffold. In the double-phase configuration, the scaffold colonization improved in comparison with the previous culture conditions. The external surface was uniformly covered by a major ECM layer. Fibroblasts partially covered the luminal side throughout the dynamic culture: cell number gradually increased reaching the stage of ECM deposition, demonstrating a higher rate of cell proliferation and migration throughout the scaffold thickness.

This evidence was supported by histological sections. Hematoxylin and eosin staining (Fig. 8) indicated that after 21 days of culture, the static configuration's outward surface had a thick layer of rounded cells; while, in the single-phase configuration, cells were elongated and organized into a compact tissue. Similarly, in the double-phase configuration, the external side was covered by many elongated cells, well organized in a dense and close matrix with rounded fibroblasts, colonizing also the scaffold thickness. Internally, the double-phase configuration seemed to present a thicker rounded-cell layer than the single-phase, which was not present at all in the static configuration. Moreover, the cross-section evidenced that no cells colonized the scaffold thickness in the static con-

dition; otherwise, in the single-phase and in double-phase, cells penetrated the entire scaffold wall. The outcome was further improved for the last dynamic culture condition, where fibroblasts formed conglomerates within the thickness.

Discussion

This study investigated a new polyol mixture for the production of PUFs as a scaffold for hollow TE, and the effect of different dynamic culture conditions on cell behavior and scaffold colonization. To this purpose, high porosity (about 90%) and high interconnectivity (>65%) are required to provide an adequate exchange of nutrient and waste products across the scaffold thickness and to promote rapid cell ingrowth and scaffold colonization (16, 17). Considering this, we were able to develop a 3D PUF porous scaffold with adequate morphological structure (porosity of 89.13%, interconnectivity higher than 80%). Preliminary biological assessment demonstrated the absence of toxic compounds released in culture media by PUF at day 1. The viability was further improved between days 3 and 7, while the DNA content depicted a similar growth trend for cells cultured both on PUF and static tissue culture plates. SEM micrographs indicated the presence of vital and proliferative cells, evidencing the ability of PUF scaffolds to promote cell adhesion and
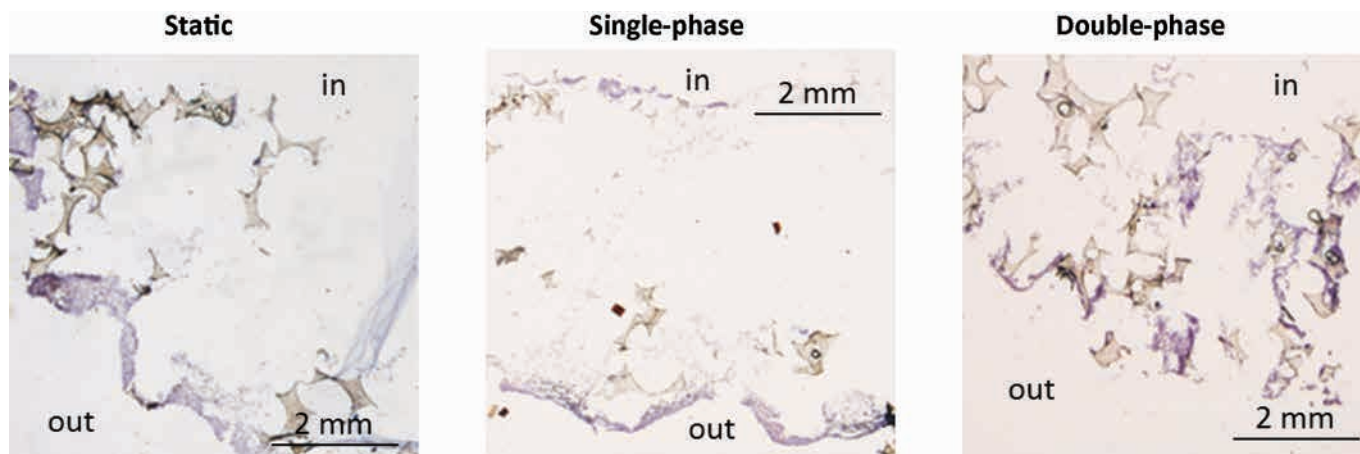
Fig. 8 - Histological images with hematoxylin and eosin staining at 21 days of culture of static, single-phase and double-phase samples. In = inner surface, out = outer surface (scale bar = 2 mm).

growth. Moreover, since pore dimension influences cells' ECM production, pore size must be higher than 68 µm; in particular, pore size in the range between 275 and 500 µm promotes tissue ingrowth (16, 17, 30, 31). These values were comparable to PUF average pore size (548 ± 120 µm). Our PUF morphological characterization demonstrated the suitability of PUF as a possible substrate for TE tubular scaffolds for hollow tissue regeneration, such as tracheas and esophagi. The mechanical characterization of the matrices produced showed Young's modulus (about 0.05 MPa), under uniaxial compression, to be comparable to soft tissues (32, 33). On the one hand, this parameter is one of the most important to be considered in TE applications, since elastic modulus, coupled with stresses and deformations, indicates the capability of the material to resist to physiological loads. On the other hand, the mechanical characterization gave us relevant information underlining the need for cell colonization and matrix deposition to enhance the performances of the material before a possible transplant. In this regard, a final direct comparison of the mechanical properties between PUF scaffold and decellularized ECM would be interesting at the end of in vitro culture, to evaluate the effect of the ECM produced and the polymeric structure.

Further, the state-of-the-art analysis demonstrated that forced convective flow throughout the scaffold wall enhances oxygen supply, nourishment and waste removal with beneficial effects on cell proliferation, scaffold colonization and ECM deposition (8, 13). In the present study, the convective flow was introduced by the longitudinal rotation, comparing 2 different dynamic conditions (single-phase and double-phase) with static controls. Our initial consideration was based on the equation of mass transport, valid for the static condition:

$$\frac{\partial c}{\partial t} = D\nabla^2 c - V \qquad \text{Eq. [4]}$$

where D is the diffusion coefficient of the considered substance through the medium, c is the molar concentration of

a substance, V is the molar rate of consumption per unit volume. A similar situation was analyzed by Asnaghi et al (8).

The introduction of longitudinal rotation added the further convective term to (Eq. [4]), due to the rotation speed, valid for both the single-phase and double-phase conditions (Eq. [5]):

$$\frac{\partial c}{\partial t} = D\nabla^2 c - V + \nabla(vc) \qquad \text{Eq. [5]}$$

where v is the velocity of "fluid" due to the rotational speed and the diffusivity coefficient D varies depending on the phase (air or culture medium).

The practical effectiveness of the longitudinal rotation in terms of biochemical and mechanical conditioning to increase cellular metabolism and scaffold colonization was demonstrated with DNA quantification and viability assay in dynamic cultures, both under the single-phase rotation and the double-phase exposure. Their higher viability and cell number in comparison with the static configuration was most likely related to the introduction of the velocity term in Equation [5]. In contrast, the absence of the convective term in the static configuration causes a lower nutrient supply, insufficient to guarantee good cell viability throughout the thickness of the 3D matrix. These quantitative results were also confirmed by SEM and histological analyses where single-phase and double-phase conditioning promoted higher cell colonization throughout the scaffold thickness. The direct comparison between single-phase and double-phase configurations indicated that the alternating exposure to air and culture medium further enhances cell metabolism and proliferation. This observation can be related to the higher value of diffusion in Equation [5]: in the single-phase, D was considered for oxygen within a fluid (culture medium) through a minimum of 0.3 cm to a maximum of 1 cm of medium; this parameter could justify the best cellular results obtained in the single-phase in comparison with static configuration. On the other hand, in the double-phase, D has 2 contributors, air and

medium, due to the longitudinal rotation and due to the level of culture medium which half cover the PUF scaffold. This gives the advantage of a faster oxygen diffusion in the thin layer of media covering the matrix when the scaffold is half-exposed to air (34). Thus, in the double-phase configuration, the scaffold surface exposed to air was subjected to an enhanced oxygenation and nourishment. On that side, cells were almost directly in contact with air, except for a thin medium layer that allows a major exchange of gases thanks to the reduced thickness of this layer (order of micrometers) in comparison with the medium barrier present in the single-phase (order of centimeters). The media convection in the scaffold improves the homogeneous distribution of the nutrients dissolved in the culture media, increasing cellular activity. Taking benefits from the increased exchange of oxygen, cell ingrowth and ECM production on the PUF pore wall surface were increased, as evidenced by the results displayed. Similar outcomes were also reached in a work by Anton et al, where the alternate contact of cells to air and medium enhanced cellular nutrients and oxygen supply (35), but a single-phase comparison was not reported.

To better support our theory, computational simulations of the 3 culture conditions should be implemented to evaluate the contribution of the double effect of convection and the alternating exposure to air and medium. The final aim will be to better understand the contribution of the different components of fluid shear and gas phases to the cellular metabolism and activities during the culture in bioreactors, both for the double-phase and single-phase conditions.

Thus, among the investigated cellular culture conditions, double-phase alternating rotation represents the optimal in vitro condition for cell proliferation, metabolism and scaffold colonization.

Conclusion

In this study, we first established that PUF morphology was adequate to promote cell adhesion and, combined with convective flow, cell movement from the external layer toward the luminal surface, highlighting the great potential of this newly developed foam. Secondly, we demonstrated the effectiveness of convective flow generated by longitudinal rotation during cell culture, coupled with double-phase exposure, for tubular 3D porous scaffolds. The alternating exposure to air and culture medium of the seeded porous scaffolds improves viability, proliferation, scaffold thickness colonization and ECM production, since the biochemical and mechanical conditioning optimizes the oxygen supply and the exchange of nutrients and waste.

In summary, alternated double-phase rotation provided the optimal biochemical and mechanical stimuli able to promote the development of functional 3D TE constructs in the rotating bioreactor developed.

Acknowledgements

Disclosures

References

1. Alwan A, Armstrong T, Bettcher D, et al. Global status report on noncommunicable diseases. Geneva, Switzerland: World Health Organization; 2011.

2. Lim SS, Vos T, Flaxman AD, et al. A comparative risk assessment of burden of disease and injury attributable to 67 risk factors and risk factor clusters in 21 regions, 1990-2010: a systematic analysis for the Global Burden of Disease Study 2010. Lancet. 2012;380(9859):2224-2260.

3. World Health Organization. The top 10 causes of death. Updated May 2014. http://www.who.int/mediacentre/factsheets/fs310/en/. Accessed May 19, 2015.

4. Nasseri BA, Ogawa K, Vacanti JP. Tissue engineering: an evolving 21st-century science to provide biologic replacement for reconstruction and transplantation. Surgery. 2001;130(5):781-784.

5. Fuchs JR, Nasseri BA, Vacanti JP. Tissue engineering: a 21st century solution to surgical reconstruction. Ann Thorac Surg. 2001;72(2):577-591.

6. Vacanti J. Tissue engineering and regenerative medicine: from first principles to state of the art. J Pediatr Surg. 2010;45(2):291-294.

7. Martin I, Simmons PJ, Williams DF. Manufacturing challenges in regenerative medicine. Sci Transl Med. 2014;6(232):232fs16.

8. Asnaghi MA, Jungebluth P, Raimondi MT, et al. A double-chamber rotating bioreactor for the development of tissue-engineered hollow organs: from concept to clinical trial. Biomaterials. 2009;30(29):5260-5269.

9. Macchiarini P, Jungebluth P, Go T, et al. Clinical transplantation of a tissue-engineered airway. Lancet. 2008;372(9655):2023-2030.

10. Carrier RL, Rupnick M, Langer R, Schoen FJ, Freed LE, Vunjak-Novakovic G. Effects of oxygen on engineered cardiac muscle. Biotechnol Bioeng. 2002;78(6):617-625.

11. Arrigoni C, Chittò A, Mantero S, Remuzzi A. Rotating versus perfusion bioreactor for the culture of engineered vascular constructs based on hyaluronic acid. Biotechnol Bioeng. 2008;100(5):988-997.

12. Marsano A, Wendt D, Quinn TM, et al. Bi-zonal cartilaginous tissues engineered in a rotary cell culture system. Biorheology. 2006;43(3-4):553-560.

13. Lin CH, Hsu SH, Huang CE, Cheng WT, Su JM. A scaffold-bioreactor system for a tissue-engineered trachea. Biomaterials. 2009;30(25):4117-4126.

14. Crowley C, Birchall M, Seifalian AM. Trachea transplantation: from laboratory to patient. J Tissue Eng Regen Med. 2015;9(4):357-367.

15. Hollister SJ. Porous scaffold design for tissue engineering. Nat Mater. 2005;4(7):518-524.

16. Tan JY, Chua CK, Leong KF, Chian KS, Leong WS, Tan LP. Esophageal tissue engineering: an in-depth review on scaffold design. Biotechnol Bioeng. 2012;109(1):1-15.

17. Mehdizadeh H, Sumo S, Bayrak ES, Brey EM, Cinar A. Three-dimensional modeling of angiogenesis in porous biomaterial scaffolds. Biomaterials. 2013;34(12):2875-2887.

18. Vikingsson L, Claessens B, Gómez-Tejedor JA, Gallego Ferrer G, Gómez Ribelles JL. Relationship between micro-porosity, water permeability and mechanical behavior in scaffolds for cartilage engineering. J Mech Behav Biomed Mater. 2015;48:60-69.

19. Stefani I, Cooper-White JJ. Development of an in-process UV-crosslinked, electrospun PCL/aPLA-co-TMC composite polymer for tubular tissue engineering applications. Acta Biomater. 2016;36:231-240.

20. Akbarzadeh R, Yousefi AM. Effects of processing parameters in thermally induced phase separation technique on porous architecture of scaffolds for bone tissue engineering. J Biomed Mater Res B Appl Biomater. 2014;102(6):1304-1315.

21. Giannitelli SM, Accoto D, Trombetta M, Rainer A. Current trends in the design of scaffolds for computer-aided tissue engineering. Acta Biomater. 2014;10(2):580-594.

22. Tresoldi C, Pellegata AF, Mantero S. Cells and stimuli in small-caliber blood vessel tissue engineering. Regen Med. 2015;10(4): 505-527.

23. Tanzi MC, Farè S, Petrini P, et al. Cytocompatibility of polyurethane foams as biointegrable matrices for the preparation of scaffolds for bone reconstruction. J Appl Biomater Biomech. 2003;1(1):58-66.

24. Gleghorn JP, Doty SB, Warren RF, Wright TM, Maher SA, Bonassar LJ. Analysis of frictional behavior and changes in morphology resulting from cartilage articulation with porous polyurethane foams. J Orthop Res. 2010;28(10):1292-1299.

25. Caracciolo PC, Thomas V, Vohra YK, Buffa F, Abraham GA. Electrospinning of novel biodegradable poly(ester urethane)s and poly(ester urethane urea)s for soft tissue-engineering applications. J Mater Sci Mater Med. 2009;20(10):2129-2137.

26. Hafeman AE, Li B, Yoshii T, Zienkiewicz K, Davidson JM, Guelcher SA. Injectable biodegradable polyurethane scaffolds with release of platelet-derived growth factor for tissue repair and regeneration. Pharm Res. 2008;25(10):2387-2399.

27. Zanetta M, Quirici N, Demarosi F, Tanzi MC, Rimondini L, Farè S. Ability of polyurethane foams to support cell proliferation and the differentiation of MSCs into osteoblasts. Acta Biomater. 2009;5(4):1126-1136.

28. Bertoldi S, Farè S, Denegri M, et al. Ability of polyurethane foams to support placenta-derived cell adhesion and osteogenic differentiation: preliminary results. J Mater Sci Mater Med. 2010;21(3):1005-1011.

29. Moore MJ, Jabbari E, Ritman EL, et al. Quantitative analysis of interconnectivity of porous biodegradable scaffolds with micro-computed tomography. J Biomed Mater Res A. 2004;71(2):258-267.

30. Wang Y, Hu J, Jiao J, et al. Engineering vascular tissue with functional smooth muscle cells derived from human iPS cells and nanofibrous scaffolds. Biomaterials. 2014;35(32):8960-8969.

31. Tsukada H, Osada H. Experimental study of a new tracheal prosthesis: pored Dacron tube. J Thorac Cardiovasc Surg. 2004;127(3): 877-884.

32. Zhang L, Gurao M, Yang KH, King AI. Material characterization and computer model simulation of low density polyurethane foam used in a rodent traumatic brain injury model. J Neurosci Methods. 2011;198(1):93-98.

33. Mansfield EG, Greene VK Jr, Auguste DT. Patterned, tubular scaffolds mimic longitudinal and radial mechanics of the neonatal trachea. Acta Biomater. 2016;33:176-182.

34. Welty JR, Wicks CE, Wilson RE, et al, eds. Fundamentals of momentum, heat, and mass transfer. 5th ed. Wiley. 2008.

35. Anton F, Suck K, Diederichs S, et al. Design and characterization of a rotating bed system bioreactor for tissue engineering applications. Biotechnol Prog. 2008;24(1):140-147.